

## Isoscalar monopole and dipole strength between 10 and 20 MeV in $^{24}\text{Mg}$ from inelastic $\alpha$ scattering at and around $0^\circ$

H. J. Lu,\* S. Brandenburg, R. De Leo,† M. N. Harakeh, T. D. Poelheken, and A. van der Woude

*Kernfysisch Versneller Instituut, 9747 AA Groningen, The Netherlands*

(Received 18 July 1985)

Differential cross sections for inelastic  $\alpha$  scattering from  $^{24}\text{Mg}$  in the region of 10–20 MeV excitation have been measured at  $E_\alpha = 120$  MeV in the angular range of  $0^\circ$ – $8^\circ$ . The strength distribution for isoscalar monopole and dipole strength in  $^{24}\text{Mg}$  between 11–20 MeV was determined.  $90 \pm 20\%$  of the  $E0$  energy-weighted sum rule and  $56 \pm 12\%$  of the  $E1$ ,  $\Delta T = 0$  energy-weighted sum rule are found to be exhausted in this excitation energy region.

The excitation of compressional modes in nuclei is an interesting topic in view of the fact that their excitation energies are related to the incompressibility of nuclear matter ( $k_\infty$ ). However, since the nuclear compression modulus  $K_A$  for finite nuclei, in addition to its dependence on  $K_\infty$ , also depends on surface, charge, and isospin symmetry effects<sup>1,2</sup> it is imperative to determine the excitation energies of the compression modes as a function of mass number in order to disentangle the various contributions.

The compressional modes predicted to lie at the lowest excitation energies are the giant monopole resonance (GMR or breathing mode) and the isoscalar giant dipole resonance (ISGDR or squeezing mode).<sup>1,3–6</sup> Little is known about the ISGDR,<sup>7–10</sup> but the existence of the GMR has been well established in nuclei with  $A > 60$ .<sup>2,11,12</sup> However, until recently only little monopole strength was observed in nuclei with  $A \leq 40$ .<sup>11,13–19</sup> In a recent experiment<sup>20</sup> we located  $\sim 23\%$  of the  $E0$ , energy-weighted sum rule (EWSR) monopole strength between 10.5–15.7 MeV and  $\sim 7\%$  of the  $E0$ , EWSR between 15.7–20 MeV in  $^{40}\text{Ca}$  from singles and  $\alpha_0$ -decay coincidence measurements for inelastic  $\alpha$  scattering at  $E_\alpha = 120$  MeV at angles around and including  $0^\circ$ . More recently, a substantial fraction ( $\sim 66\%$ ) of the  $E0$ , EWSR was identified in  $^{28}\text{Si}$  with a centroid energy of  $E_x = 17.9$  MeV from an inelastic  $\alpha$ -scattering experiment,<sup>21</sup> including a measurement at  $\theta = 0^\circ$ .

In this paper we present data for inelastic  $\alpha$  scattering from  $^{24}\text{Mg}$ . This nucleus was chosen because it shows structure up to 20 MeV excitation energy. Since the angular distributions at and around  $0^\circ$  are also characteristic<sup>22</sup> for isoscalar dipole transfer the angular range for which measurements were performed was from  $0^\circ$ – $8^\circ$ , covering both the maximum of the angular distribution of  $L = 0$  at  $0^\circ$  and of  $L = 1$ ,  $\Delta T = 0$  at  $4^\circ$ .

The 120 MeV analyzed alpha beam from the KVI AVF cyclotron was used to bombard a  $^{24}\text{Mg}$  target of  $\sim 380$   $\mu\text{g}/\text{cm}^2$  thickness isotopically enriched to 99.5%. The target was freshly prepared to minimize oxygen and carbon contamination. The inelastically scattered alpha particles were detected in the QMG/2 magnetic spectrograph.<sup>23</sup> The experiment consisted of two sets of measurements. In one measurement the spectrograph was set at  $\theta_{\text{lab}} = 1.5^\circ$  with a full horizontal opening angle  $\Delta\theta = 6^\circ$  and with a vertical opening angle of  $\Delta\theta = 2.4^\circ$ . In this way differential cross sections ranging from  $0$ – $4.5^\circ$  could be measured in one setting. In this  $0^\circ$  setup the 52 cm long detection system<sup>24</sup> was used for the detection and identification of the inelastically

scattered  $\alpha$  particles in the focal plane of the spectrograph. Other experimental details are similar to those published in Ref. 20. In this setup the excitation energy region of 11–20 MeV in  $^{24}\text{Mg}$  was covered. Differential cross sections were reconstructed for the angular intervals  $-1.5^\circ < \theta < 1.5^\circ$ ,

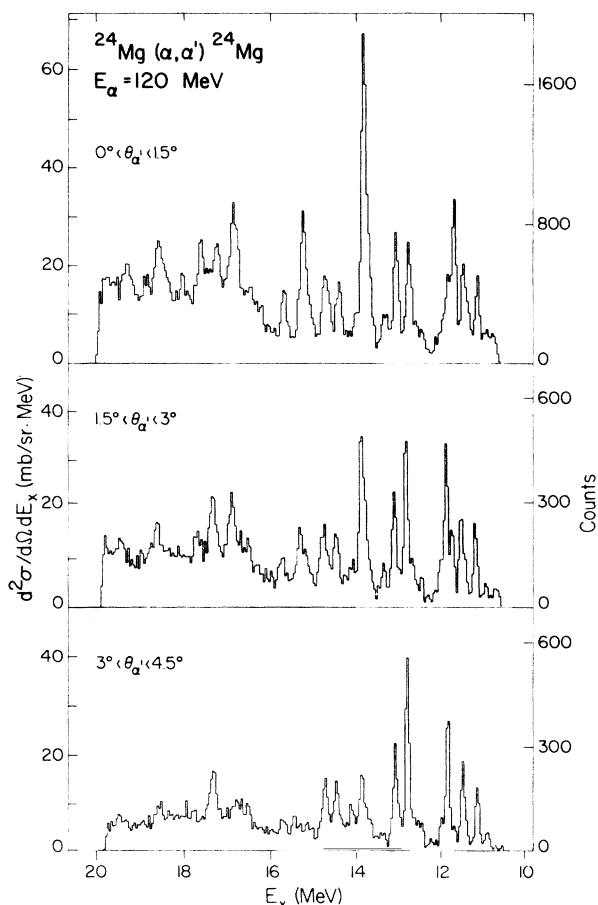


FIG. 1. Spectra for inelastic  $\alpha$  scattering from  $^{24}\text{Mg}$  taken at  $E_\alpha = 120$  MeV and for very forward angles. The spectra were generated by "ray-tracing procedure" from the singles data taken with the QMG/2 spectrograph which was set at  $\theta = 1.5^\circ$  with a horizontal opening angle of  $6^\circ$  and a vertical opening angle of  $2.4^\circ$ , thus also including  $0^\circ$  scattering angle. The angular intervals for which the spectra were generated are indicated in the figure. The spectra show structure up to 20 MeV.

$1.5^\circ < \theta < 3^\circ$ , and  $3^\circ < \theta < 4.5^\circ$  with an experimentally checked<sup>25</sup> resolution of  $\Delta\theta = 0.7^\circ$ .

The instrumental background due to beam halo and slit scattering could be effectively discriminated against by determining for each event the time of flight, the horizontal angle of incidence in the focal plane, and the vertical position. This technique will be described in a forthcoming paper.<sup>25</sup> The spectra from which this instrumental background has been eliminated are shown in Fig. 1. In these spectra two interesting features are observed immediately: (i) They show structure up to 20 MeV. (ii) There are structures of which the angular distributions drop sharply as a function of scattering angle indicative of the presence of  $L = 0$  excitation.

In the second set of measurements, the beam was stopped in a Faraday cup inside the scattering chamber. The spectrograph was set at angles  $\theta = 5^\circ, 6^\circ$ , and  $8^\circ$ , with horizontal and vertical opening angles of  $1.5^\circ$  and  $2.4^\circ$ , respectively. In this case, the 120 cm long detection system of the spectrograph was used, which is similar in construction and operation to the 52 cm long detection system except for its length. Essentially the spectra obtained (not shown here) are of the same quality as those obtained with the spectrograph at  $0^\circ$  and shown in Fig. 1.

Angular distributions obtained for some of the excitation energy intervals listed in Table I and without any background subtraction are shown in Fig. 2. The assumption that no physical or instrumental background is present is justified on the basis of angular correlation measurements,<sup>25</sup> where not only no evidence for quasielastic knockout continuum could be observed for this excitation energy range

TABLE I. Multipole strength distribution in percentages of respective ESWR's.

Excitation energy intervals (MeV)	$L = 0$	$L = 1$	$L = 2$	$L = 4$
11.23-11.58	0.73	1.9	3.3	...
11.59-11.74	1.8	...	0.16	...
11.75-11.87	...	2.5	...	...
11.88-12.30	...	...	1.1	...
12.31-12.65	...	0.94	1.2	...
12.66-12.88	...	2.8	3.2	...
12.89-13.23	0.97	2.2	2.3	...
13.24-13.52	0.75	...	0.61	...
13.53-13.97	7.7	...	2.0	...
13.98-14.25	0.19	1.2	...	2.7
14.26-14.56	0.99	1.5	2.4	...
14.57-14.98	2.1	2.0	2.9	...
14.99-15.51	5.7	0.78	2.4	...
15.52-15.93	2.4	1.2	1.5	...
15.94-16.54	4.8	2.0	3.2	...
16.55-17.04	10.2	2.9	3.8	...
17.05-17.46	7.8	5.1	...	1.6
17.47-17.80	5.4	2.6	6.4	...
17.81-18.24	5.6	4.2	3.1	...
18.25-18.90	13.5	6.3	5.9	...
18.91-19.51	11.0	8.5	...	4.3
19.52-19.99	8.8	7.0	5.4	...
Total	$90 \pm 20$	$56 \pm 12$	$51 \pm 11$	8.6

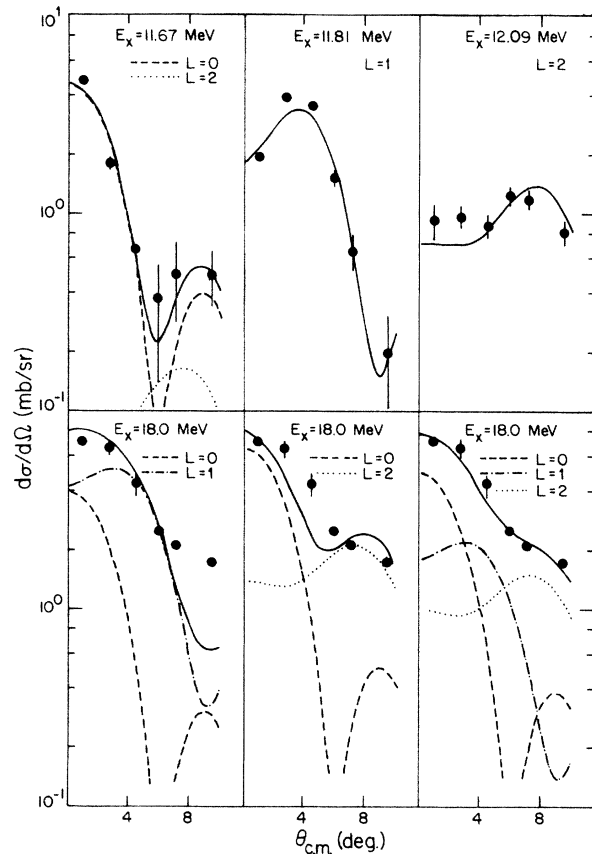


FIG. 2. Angular distributions for few representative excitation energy intervals (listed in Table I) in  $^{24}\text{Mg}$  in the measured excitation energy region. In the first row angular distributions are shown for intervals which are indicative of pure  $L = 1$  and  $L = 2$  transfers centered at  $E_x = 11.81$  and  $12.09$  MeV, respectively, and almost pure  $L = 0$  transfer at  $E_x = 11.67$  MeV. In the second row the angular distribution for the structure centered around  $18.02$  MeV, which has a strong  $L = 0$  contribution, is shown. The three fits indicate the sensitivity of the measured forward angular distribution to contributions of various multipolarities (see text for more details).

and at these forward scattering angles, but which also showed that the full singles cross section could be recovered from the partial cross sections of the various decay channels, thus showing the absence of an instrumental background. The first row in Fig. 2 shows angular distributions taken from the low excitation energy region where sharp peaks are observed, while the second row shows the angular distribution for the interval centered around the structure at  $18.02$  MeV. In this last region of excitation, resonances overlap and angular distributions are more complex.

The error bars shown in Fig. 2 are statistical. Absolute uncertainties in the differential cross sections are of the order of 10%. They are normalized by comparing measured elastic cross sections to optical model calculations. Comparing differential cross sections for some known peaks in the excitation energy region 11-16 MeV with those determined by van der Borg, Harakeh, and van der Woude<sup>9</sup> showed a good agreement.

The differential cross sections were compared to distorted wave Born approximation (DWBA) calculations. Optical model potential parameters used in Ref. 9 were also used

here. In these DWBA calculations, transition potentials for  $L \geq 2$  were taken to be of the usual surface type  $-R(dU/dr)$ , while for  $L=0$  the monopole transition potential (version I) of Satchler<sup>26</sup> and for isoscalar  $L=1$  the transition potential of Harakeh and Dieperink<sup>22</sup> were used. The calculation for the isoscalar monopole and dipole excitations which do not involve Coulomb excitation were performed using the program DWUCK.<sup>27</sup> However, for  $L \geq 2$  transitions the program ECIS<sup>28</sup> was used because of its better handling of Coulomb excitation, which is rather important for small scattering angles. The deformation parameters for the real, imaginary, and Coulomb parts of the transition potential were adjusted to yield the same multipole radial moments. This was separately performed for the various multipole transitions according to the prescription of Ref. 29. In the first row of Fig. 2, predicted DWBA angular distributions are compared with the differential cross sections for intervals centered at  $E_x=11.81$  and  $12.09$  MeV, which clearly are due to pure  $L=1$  and  $L=2$  transitions, and for an interval centered at  $E_x=11.67$  MeV, which is due to an almost pure  $L=0$  transition with possibly a small contribution from a  $L=2$  transition. The theoretical angular distributions were averaged over an opening angle  $\Delta\theta=1.5^\circ$  horizontally and  $\Delta\theta=2.4^\circ$  vertically before comparison with the experimental cross sections. The good agreement between the data and the DWBA calculations gives us confidence in our comparison for the higher excitation energy region.

In general, angular distributions were fitted in a  $\chi^2$  procedure with a sum of different  $L$  transfers. In the second row of Fig. 2, this is illustrated for the excitation energy interval centered around  $18.02$  MeV. First a fit with only a sum of  $L=0$  and  $L=1$  was tried. Although a good fit is obtained for the first three data points, the points at larger angles could not be fitted without assuming a contribution from  $L \geq 2$  transfer. On the other hand, a fit with a sum of  $L=0$  and  $L=2$  transfer fails to reproduce the rise of the data points at  $\theta=2.25^\circ$  and  $3.75^\circ$ , which is very characteristic for  $L=1$  transfer. In general, one can fit the data in the region  $E_x=16$ – $20$  MeV by the sum of  $L=0$ ,  $L=1$ , and some higher  $L$ . We have consistently used  $L=2$ , since it gave slightly, though not very significantly, better  $\chi^2$  than higher  $L$  admixtures. Such a fit is shown in the right lower part of Fig. 2 and it is seen to fit the data nicely. Only in three cases did a fit with  $L=4$  in addition to  $L=0$  and  $L=1$  give a significantly better  $\chi^2$  than with  $L=2$  (see Table I). Below  $16$  MeV, it was usually enough to use one or two  $L$  transfers to fit the data.

The deformation parameters were obtained from the  $\chi^2$  fitting procedure and were converted to transition rates  $B(EL)$ 's by using<sup>29</sup> the radial multipole moments of the real part of the optical potential. This procedure gives<sup>30</sup> the correct  $B(EL)$  values for known transitions to low-lying states in  $^{24}\text{Mg}$ . These were converted to fractions of the respective EWSR, which are listed in Table I, which also shows the total amounts of isoscalar  $E0$ ,  $E1$ , and  $E2$  strengths observed in this experiment between  $11$ – $20$  MeV. A number of remarks can be made. First, the amount and distribution of  $E2$  strength is in complete agreement with the results obtained earlier from large angle single-arm and coincidence measurements.<sup>9,19</sup> If we had subtracted some nuclear or instrumental continuum from the angles  $\theta_{\text{lab}}=5^\circ$ ,  $6^\circ$ , and  $8^\circ$ , where such a continuum "appears" to exist, then these three data points would have been lowered for the excitation energy region  $16$ – $20$  MeV. This would have led to substantially less  $L=2$  strength in disagreement with all previous measurements,<sup>9</sup> whereas the deduced monopole strength remains hardly affected and the dipole strength is slightly affected. Second, for the first time an appreciable amount of isoscalar dipole strength ( $56 \pm 12\%$   $\Delta T=0$ ,  $E1$  EWSR) has been observed in light nuclei. Finally, the observed  $E0$  strength of  $\sim 90 \pm 20\%$  EWSR indicates that most of the  $E0$  strength has been observed with very little left over to be found above  $20$  MeV.

The centroid energy of the observed  $E0$  strength in  $^{24}\text{Mg}$  in this experiment is  $17.2$  MeV. Since the observed  $E0$  strength almost exhausts the sum rule, this centroid energy was used along with all the available experimental information on the excitation energy of monopole resonances for those nuclei for which the bulk of the GMR was observed<sup>2,21</sup> and excluding all results for deformed nuclei for which the two GMR components were not observed to fit the parameters in the general formula [Eq. (5) of Ref. 2] for the excitation energy of the monopole resonance. Using the values for  $K_{\text{surf}}$  and  $K_{\text{sym}}$  obtained by Blaizot<sup>1</sup> from a simple estimate as starting values, we obtain the following parameters:  $K_\infty=253 \pm 16$  MeV,  $K_{\text{surf}}=-488 \pm 56$  MeV, and  $K_{\text{sym}}=-285 \pm 448$  MeV.

This work has been performed as part of the research program of the Stichting voor Fundamenteel Onderzoek der Materie (FOM), with financial support of the Nederlandse Organisatie voor Zuiver Wetenschappelijk Onderzoek (ZWO).

\*Permanent address: Institute of Atomic Energy, Beijing, Peoples Republic of China.

†Permanent address: Dipartimento di Fisica dell'Università di Bari, Bari, Italy.

<sup>1</sup>J. P. Blaizot, Phys. Rep. **64**, 171 (1980).

<sup>2</sup>M. Buenerd, *Proceedings of the International Symposium on Highly Excited States and Nuclear Structure, Orsay, France, 1983* [J. Phys. (Paris) Colloq. **45**, C4-115 (1984), and references therein].

<sup>3</sup>A. Bohr and B. R. Mottelson, *Nuclear Structure* (Benjamin, Reading, MA, 1975), Vol. II, and references therein.

<sup>4</sup>T. J. Deal, Nucl. Phys. **A217**, 210 (1973).

<sup>5</sup>N. Van Giai and H. Sagawa, Nucl. Phys. **A371**, 1 (1981).

<sup>6</sup>R. De Haro, S. Krewald, and J. Speth, Nucl. Phys. **A388**, 265 (1982).

<sup>7</sup>H. P. Morsch, M. Rogge, P. Turek, and C. Mayer-Böricke, Phys. Rev. Lett. **45**, 337 (1980).

<sup>8</sup>C. Djalali, N. Marty, M. Morlet, and A. Willis, Nucl. Phys. **A380**, 42 (1982).

<sup>9</sup>K. van der Borg, M. N. Harakeh, and A. van der Woude, Nucl. Phys. **A365**, 243 (1981), and references therein.

<sup>10</sup>B. Bonin *et al.*, Nucl. Phys. **A430**, 349 (1984).

<sup>11</sup>D. H. Youngblood *et al.*, Phys. Rev. C **23**, 1997 (1981), and references therein.

<sup>12</sup>J. Speth and A. van der Woude, Rep. Prog. Phys. **44**, 719 (1981), and reference therein.

<sup>13</sup>M. Buenerd *et al.*, Phys. Rev. Lett. **45**, 1667 (1980).

<sup>14</sup>D. Lebrun *et al.*, Phys. Lett. **97B**, 358 (1980).

<sup>15</sup>Y.-W. Lui *et al.*, Phys. Rev. C **24**, 884 (1981).

- <sup>16</sup>H. Rost *et al.*, Phys. Lett. **88B**, 51 (1979).  
<sup>17</sup>A. Willis *et al.*, Nucl. Phys. **A344**, 137 (1980).  
<sup>18</sup>T. Yamagata *et al.*, Phys. Rev. Lett. **40**, 1628 (1978).  
<sup>19</sup>F. Zwarts, A. G. Drentje, M. N. Harakeh, and A. van der Woude, Phys. Lett. **125B**, 123 (1983); Nucl. Phys. **A439**, 117 (1985).  
<sup>20</sup>S. Brandenburg *et al.*, Phys. Lett. **130B**, 9 (1983).  
<sup>21</sup>Y.-W. Lui *et al.*, Phys. Rev. C **31**, 1643 (1985).  
<sup>22</sup>M. N. Harakeh and A. E. L. Dieperink, Phys. Rev. C **23**, 2329 (1981).  
<sup>23</sup>A. G. Drentje, H. A. Enge, and S. B. Kowalski, Nucl. Instrum. Methods **122**, 485 (1974).  
<sup>24</sup>J. C. Vermeulen *et al.*, Nucl. Instrum. Methods **180**, 93 (1981).  
<sup>25</sup>S. Brandenburg *et al.* (unpublished).  
<sup>26</sup>G. R. Satchler, Part. Nucl. **5**, 105 (1973).  
<sup>27</sup>P. D. Kunz, program DWUCK (unpublished).  
<sup>28</sup>J. Raynal, program ECIS (unpublished).  
<sup>29</sup>M. N. Harakeh, Kernfysisch Versneller Instituut der Rijksuniversiteit Report No. 77i, 1981 (unpublished); R. S. Mackintosh, Nucl. Phys. **A266**, 379 (1976).  
<sup>30</sup>M. Pignanelli, S. Micheletti, R. De Leo, S. Brandenburg, and M. N. Harakeh, Phys. Rev. C (to be published).